

Reformulation of Dynamic Manipulability Ellipsoid for Robotic Manipulators

P. Chiacchio, S. Chiaverini, L. Sciavicco, and B. Siciliano

Dipartimento di Informatica e Sistemistica
Università degli Studi di Napoli "Federico II"
via Claudio 21, 80125 Napoli, Italy

Abstract

A reformulation of dynamic manipulability ellipsoid for robotic manipulators is established in this paper. This ellipsoid is a common tool in robotics to measure the ability of a manipulator to produce arbitrary accelerations of the end effector for a given set of torques at the joints. As opposed to the original approach where gravitational forces were imputed to compress the volume of the ellipsoid, here we show that the effect of gravity can be taken into account by translating the center of the ellipsoid without affecting its volume. Further, we characterize the ellipsoid for redundant manipulators by investigating the properties of the manipulator Jacobian involved in the core of the ellipsoid. Numerical case studies are developed.

1. Introduction

The concept of manipulability was introduced some years ago as an effective means to perform task-space analysis of robotic manipulators [1]. The idea is to set up quantitative measures of the ease of arbitrarily changing the location of the end effector by acting on the joints. This may be advantageous both for optimal design of manipulator structures and for determination of optimal postures for executing a given task. The key at the basis of the definition of such ellipsoids is the manipulator Jacobian which describes the mapping from the joint space to the task space.

If we are simply interested to studying the differential kinematics relationship, together with the statics relationship that can be derived in force of the duality principle, kineto-static manipulability ellipsoids can be defined [2]. For each configuration of the arm, the velocity ellipsoid gives an index of the ability of performing end-effector velocities along each task-space direction for a given set of joint velocities. Dually, the force ellipsoid gives an index of the ability of performing end-effector forces along each task-space direction for a given set of joint torques. It can be shown that the principal axes of the two ellipsoids coincide,

whereas the lengths of the axes are in inverse proportion. These properties have later been refined in [3] where it is keenly proposed to view the manipulator as a mechanical transformer from the joint space to the task space, leading to the definition of suitable task compatibility indices. Also, several dexterity measures can be derived for the matrix constituting the core of the ellipsoid which can be analyzed as a function of joint configurations [4]. A more recent work characterizes translational and rotational manipulability for typical manipulators having a shoulder, an elbow, and a wrist [5].

On the other hand, in all those cases where the arm dynamics cannot be neglected, it is necessary to consider the dynamic manipulability ellipsoid [6] which gives a measure of the ability of performing end-effector accelerations along each task-space direction for a given set of joint torques. Related to this concept is the generalized inertia ellipsoid [7] which gives an index of the ability of changing end-effector velocities along each task-space direction for a given value of kinetic energy. Other manipulability measures have recently been introduced in the literature including the coupling coefficients of robot dynamic model [8] which characterize the structural coupling of the dynamic equations of motion, the acceleration radius [9] which is defined as the minimum upper bound of the magnitude of end-effector accelerations over the entire manipulator workspace, and the dynamic conditioning index [10] which is defined as the least-squares difference between the generalized inertia matrix and an ideal isotropic matrix for the same manipulator.

One limitation of all the above approaches is that only the inertia matrix is investigated, and the gravitational force vector is left out of the analysis, with the exception of the original work [6] which indeed took gravity into account in the derivation of the dynamic manipulability ellipsoid. We argue that the effects of gravity are at least of the same importance as that of inertia in performing a dynamic analysis of robotic manipulators. This has recently motivated us to reconsider

the whole matter from a critical standpoint and conducted us to derive, what we believe, a more correct formulation of the dynamic manipulability ellipsoid, as compared to the ellipsoid defined in [6].

In particular, this work is intended to demonstrate that, when gravitational forces are properly embedded into the derivation of the dynamic manipulability ellipsoid, these do not cause any compression in the volume of the ellipsoid, as shown in [6] instead, but they just produce a translation of its center which in general occurs along all task-space directions.

Furthermore, we extend the new formulation to kinematically redundant structures because they constitute the most interesting class of manipulators for employing these manipulability measures. The extra degrees of freedom, in fact, can be conveniently exploited to reconfigure the arm in a more dexterous posture to execute the assigned task. In this case, we emphasize the properties of the manipulator Jacobian involved in the derivation by showing that only the components of the accelerations which are in the range space of the Jacobian transpose are mapped into the core of the defined ellipsoid.

A number of significant case studies illustrate the correctness and functionality of the approach for 'easy-to-understand' planar arms.

2. Dynamic Manipulability Ellipsoid

It is well-known that the dynamic model of a robotic manipulator in the joint space can be written in the closed form

$$\mathbf{M}(\mathbf{q})\ddot{\mathbf{q}} + \mathbf{c}(\mathbf{q}, \dot{\mathbf{q}}) + \mathbf{g}(\mathbf{q}) + \mathbf{J}^T(\mathbf{q})\mathbf{h} = \mathbf{f} \quad (1)$$

where \mathbf{q} is the $(n \times 1)$ vector of joint displacements, \mathbf{M} is the $(n \times n)$ symmetric, positive-definite matrix of inertia, \mathbf{c} is the $(n \times 1)$ vector of Coriolis and centrifugal forces, \mathbf{g} is the $(n \times 1)$ vector of gravitational forces, \mathbf{f} is the $(n \times 1)$ vector of joint torques,* \mathbf{h} is the $(m \times 1)$ vector of end-effector forces (due either to contact with the environment or to a carried payload), and \mathbf{J} is the $(m \times n)$ Jacobian matrix describing the mapping from the n -dimensional joint space to an m -dimensional task space of interest, with $m \leq n$. This mapping can be written as

$$\mathbf{v} = \mathbf{J}(\mathbf{q})\dot{\mathbf{q}} \quad (2)$$

where \mathbf{v} is the $(m \times 1)$ vector of end-effector velocities described with respect to a constant reference frame (usually chosen at the basis of the arm). If $m < n$,

* Notice that by the terms 'force' and 'torque' we mean actual generalized forces.

the manipulator is said to be kinematically redundant. The above mapping can be differentiated with respect to time to yield the relationship between joint accelerations and end-effector accelerations, which is of interest for dynamic analysis,

$$\mathbf{a} = \mathbf{J}(\mathbf{q})\ddot{\mathbf{q}} + \dot{\mathbf{J}}(\mathbf{q})\dot{\mathbf{q}}. \quad (3)$$

For the purpose of the present work, we restrict our study to considering only translational end-effector accelerations, thus $m \leq 3$. For typical manipulators formed by an arm and a (spherical) wrist, in fact, the dominant part of the dynamics is associated with the arm. Also, in the case when end-effector forces are generated by a carried payload, we can express the dynamic equations of the payload in the closed form

$$m_p \mathbf{a} + \mathbf{g}_p = \mathbf{h} \quad (4)$$

where m_p is the payload mass and \mathbf{g}_p is the $(m \times 1)$ vector of gravitational forces of payload.

The goal is to study the manipulability of the arm in terms of the mapping between joint torques and end-effector accelerations.

Similarly to the formulation in [6], we regard the case when the arm is standing still ($\dot{\mathbf{q}} = \mathbf{0}$) as the relevant case for analyzing dynamic manipulability. This implies that we neglect the effect of Coriolis and centrifugal terms in (1), i.e. $\mathbf{c}(\mathbf{q}, \dot{\mathbf{q}}) = \mathbf{0}$. Accordingly, in (3) it is $\dot{\mathbf{J}}(\mathbf{q})\dot{\mathbf{q}} = \mathbf{0}$.

Under the above assumptions, on reduction of (1), (3) and (4), the following equations can be obtained — where the dependence on \mathbf{q} is omitted for notation compactness —

$$\mathbf{B}\ddot{\mathbf{q}} + \mathbf{p} = \mathbf{f} \quad (5)$$

where $\mathbf{B} = (\mathbf{M} + m_p \mathbf{J}^T \mathbf{J})$ is the total symmetric, positive-definite inertia matrix and $\mathbf{p} = \mathbf{g} + \mathbf{J}^T \mathbf{g}_p$ are the total gravitational forces resulting for the system consisting of the arm and payload. Also, equation (3) simplifies to

$$\mathbf{a} = \mathbf{J}\ddot{\mathbf{q}} \quad (3')$$

which, together with (5), will yield the sought mapping.

2.1. Non-Redundant Manipulators

Let us first consider the case of non-redundant manipulators ($m = n$). Solving (3') for $\ddot{\mathbf{q}}$ gives

$$\ddot{\mathbf{q}} = \mathbf{J}^{-1} \mathbf{a} \quad (6)$$

where it has been assumed that the arm is not in a kinematically singular configuration, i.e. $\det(\mathbf{J}) \neq 0$. Then, plugging (6) into (5) results into

$$\mathbf{B}\mathbf{J}^{-1} \mathbf{a} + \mathbf{p} = \mathbf{f}. \quad (7)$$

At this point, it is opportune to normalize the joint torques to account for the different torque limits on the joint actuators. Let then $f_{i,\max}, i = 1, \dots, n$ denote the maximum (positive) driving torque at each joint of the arm; without loss of generality, we suppose that the upper and lower torque limits are of equal magnitude. The normalized torque vector can be introduced as

$$\tilde{\mathbf{f}} = \mathbf{T}\mathbf{f} \quad (8)$$

where $\mathbf{T} = \text{diag}(T_1, \dots, T_n)$ with $T_i = 1/f_{i,\max}, i = 1, \dots, n$.

The unit sphere in the space of normalized joint torques

$$\tilde{\mathbf{f}}^T \tilde{\mathbf{f}} = 1 \quad (9)$$

maps onto the ellipsoid in the task space of end-effector accelerations

$$(\mathbf{a} + \mathbf{J}\mathbf{B}^{-1}\mathbf{p})^T \mathbf{J}^{-T} \mathbf{B} \mathbf{T}^2 \mathbf{B} \mathbf{J}^{-1} (\mathbf{a} + \mathbf{J}\mathbf{B}^{-1}\mathbf{p}) = 1 \quad (10)$$

which is defined here as the *dynamic manipulability ellipsoid* for the arm and payload. Notice that we have properly factored out the term $\mathbf{B}\mathbf{J}^{-1}$ to evidence the vector \mathbf{a} .

It can be recognized that the core of the ellipsoid $\mathbf{J}^{-T} \mathbf{B} \mathbf{T}^2 \mathbf{B} \mathbf{J}^{-1}$, which depends on inertial and geometrical characteristics of the system, uniquely determines the size and the principal axes of the ellipsoid. Noticeably, when the Jacobian is singular, it is not possible to compute $\ddot{\mathbf{q}}$ as in (6), because one — or more for multiple singularities — direction of task-space accelerations cannot be accomplished; in this occurrence, the use of a pseudoinverse of \mathbf{J} is required, leading to the derivation of an ellipsoid in a suitable subspace of the original task space.

On the other hand, the vector $-\mathbf{J}\mathbf{B}^{-1}\mathbf{p}$, due to gravity, produces a pure translation of the ellipsoid with respect to the origin of the reference frame. In fact, by rewriting (7) in the form

$$\mathbf{a} = \mathbf{J}\mathbf{B}^{-1}(\mathbf{f} - \mathbf{p}), \quad (11)$$

it is easily understood that the end-effector acceleration vector for a given configuration is obtained by superposition of the contributions of joint torques and gravity; the latter contribution is fixed for each given configuration of the system, and thus produces a fixed displacement on each acceleration vector due to the joint torques. Moreover, by setting $\mathbf{f} = \mathbf{0}$ in (11), it is seen that the vector $-\mathbf{J}\mathbf{B}^{-1}\mathbf{p}$ represents the end-effector acceleration vector induced by gravity acting on the whole system when no joint torques are applied. Notice that, because of the kinematic

constraints imposed by the manipulator structure on its different inertial components, the system performs non-isotropically; this is the reason why, in general, the vector $-\mathbf{J}\mathbf{B}^{-1}\mathbf{p}$ is not aligned with the direction of the gravitational field.

This result is in contrast with the formulation developed in [6], where the absolute value of gravitational load was subtracted by the torque limit at each joint; here, we argue that such description always penalizes the available torques in the joint space, and does not properly describe the effects of gravity on the possible end-effector accelerations. With our approach, instead, it is possible to account for the effects of gravity along task-space directions in a more correct manner.

Let us consider, for instance, only the effect of a payload mass; it is quite natural to expect that, beyond a certain value thereof, it is no longer possible to accelerate the end effector along the upward direction while is certainly possible to accelerate it downwards. On the other hand, if one would adopt the other formulation [6], the size of the ellipsoid would progressively reduce leading to the result that it is not possible to accelerate the end effector in any direction of the task space.

2.2. Redundant Manipulators

Let us now consider the case of redundant manipulators ($m < n$). This time, a unique solution to (3') cannot be found; in fact, the matrix \mathbf{J} possesses a non-empty null space of dimension $(n - m)$, under the assumption that $\text{rank}(\mathbf{J}) = m$, and the general solution is given by

$$\ddot{\mathbf{q}} = \mathbf{J}^\dagger \mathbf{a} + [\mathbf{I} - \mathbf{J}^\dagger \mathbf{J}] \ddot{\mathbf{q}}_0 \quad (12)$$

where \mathbf{J}^\dagger denotes the Moore-Penrose pseudoinverse giving the minimum-norm solution and $[\mathbf{I} - \mathbf{J}^\dagger \mathbf{J}]$ is the operator projecting onto the null space of \mathbf{J} . Therefore, there exists a set of joint accelerations $\ddot{\mathbf{q}}_0$ which do not produce any acceleration at the end effector.

We take, however, only joint accelerations which are in the range space of \mathbf{J}^T — the orthogonal complement to the null space of \mathbf{J} — because we want to characterize the mapping from the joint torque space to the end-effector acceleration task space; then we consider

$$\ddot{\mathbf{q}} = \mathbf{J}^\dagger \mathbf{a} \quad (12')$$

that, plugged into (5), results into

$$\mathbf{B}\mathbf{J}^\dagger \mathbf{a} + \mathbf{p} = \mathbf{f}. \quad (13)$$

We are now ready to derive the dynamic manipulability ellipsoid in this case. In fact, the unit sphere in the

space of normalized joint torques in (9) maps onto the ellipsoid in the task space of end-effector accelerations

$$(\mathbf{a} + \mathbf{J}\mathbf{B}^{-1}\mathbf{p})^T \mathbf{J}^\dagger \mathbf{B}^T \mathbf{B} \mathbf{J}^\dagger (\mathbf{a} + \mathbf{J}\mathbf{B}^{-1}\mathbf{p}) = 1. \quad (14)$$

We believe that some considerations on the formulation of the ellipsoid in this case are in order. In particular, it might be argued that it is improper to factor out the term $\mathbf{B}\mathbf{J}^\dagger$ since $\mathbf{J}^\dagger \mathbf{J} \neq \mathbf{I}$. Observing that $\mathbf{J}^\dagger \mathbf{J}$ can be rewritten as $\mathbf{I} - [\mathbf{I} - \mathbf{J}^\dagger \mathbf{J}]$, we have in turn neglected the joint acceleration components given by $\mathbf{B}^{-1}\mathbf{p}$ which are in the null space of \mathbf{J} . This is in agreement with the former choice of considering only joint accelerations mapped by the range space of \mathbf{J} onto the task space.

Further insight about this issue can be gained by considering the intermediate mapping from joint torques onto joint accelerations. In fact, the unit sphere in (9) can also be mapped onto the ellipsoid in the n -dimensional space of joint accelerations

$$(\ddot{\mathbf{q}} + \mathbf{B}^{-1}\mathbf{p})^T \mathbf{B}^T \mathbf{B} (\ddot{\mathbf{q}} + \mathbf{B}^{-1}\mathbf{p}) = 1. \quad (15)$$

In order to pass from the joint acceleration space to the lower m -dimensional task acceleration space, we need to apply the mapping \mathbf{J} . With this operation, all the vectors in the joint space with equal components in the range space of \mathbf{J}^T are treated in the same way. In force of this, the ellipsoid defined in (14) is actually the image of the projection, along the direction of the null space of \mathbf{J} , of the ellipsoid in (15) on the subspace spanned by the range of \mathbf{J}^T . Therefore, the sole components of the vector $\mathbf{B}^{-1}\mathbf{p}$ — representing the displacement of the ellipsoid induced by gravitational loads — to be considered are those orthogonal to the null space of \mathbf{J} . Figure 1 attempts to clarify this concept for the case of $n = 3$ and $m = 2$.

3. Case Studies

In this section, we develop a number of case studies in order to illustrate the concepts presented above. Two- and three-degree-of-freedom planar manipulators are considered, with or without a payload; the manipulators operate in a two-dimensional task space for which a reference frame is chosen so that the vector \mathbf{g}_p can be written as $(0 \quad -m_p g_0)^T$, being g_0 the positive value of gravity acceleration. For each case study, the selected manipulator configuration and the corresponding dynamic manipulability ellipsoids are reported; for easeness of comparison, the ellipsoids in each figure are drawn in the same scale.

Initially, we have considered a two-degree-of-freedom manipulator whose parameters in SI units are: $l_1 =$

$l_2 = 1$, $l_{c1} = l_{c2} = 0.5$, $m_1 = 20$, $m_2 = 10$, $I_1 = 20/12$, $I_2 = 10/12$, $f_{1,\max} = 600$, $f_{2,\max} = 200$, where l_i is the link length, l_{ci} is the distance of the link center of mass from the joint, m_i is the link mass, I_i is the link moment of inertia about the joint axis. Notice that the given inertial parameters correspond to a manipulator whose links have uniform mass distribution.

In the first case study, the assigned configuration is $\mathbf{q} = (60 \quad -120)^T$ deg. We have considered four different situations: with or without gravity, with or without a payload of 5 kg applied at the end effector. The resulting ellipsoids are plotted in Fig. 2. It can clearly be seen that the effect of gravity is a pure translation of the ellipsoid's center whilst the directions of its axes and its size remain unchanged, as anticipated in theory. The presence of a payload has the major effect to reduce the size of the ellipsoid and change the orientation of its axes. It is worth noticing that the translation of the ellipsoid center is different with respect to the case in which the manipulator is unloaded; more specifically, the translation is reduced when a payload is applied. This phenomenon could sound strange, since a larger gravitational load might be expected to produce a larger translation of the ellipsoid downwards. To gain insight in the combined effect of gravity and load at the end effector, consider a single link manipulator whose mass m is concentrated at the link center (i.e. $l_c = l/2$, $I = 0$). When the link is unloaded, the acceleration at the tip due to gravity acting on the center of mass of the link is twice as much as the one produced at the center of mass itself. This occurs because a pure geometric relationship ($l/l_c = 2$) relates the tip of the link to its center of mass. If a payload M is applied, the center of mass of the system 'link+payload' moves towards the tip of the link depending on the ratio between the load and the link mass ($l'_c = \frac{1 + 2M/m}{1 + M/m} l_c > l_c$ for $M > 0$); as a consequence, the acceleration at the tip is obtained multiplying the acceleration at the center of mass by the factor $l/l'_c = 2 \frac{1 + M/m}{1 + 2M/m}$, which decreases from 2 to 1 when the ratio M/m grows from 0 to ∞ .

For the second case study, we have selected a different configuration, namely $\mathbf{q} = (70 \quad -50)^T$ deg, with no payload. In Fig. 3 the ellipsoids respectively derived with the method in [6] and with our approach are compared: It is quite evident that with the former the size of the ellipsoid is reduced in force of an *a priori* penalization of torques in the joint space, whereas with the latter the effects of gravity are correctly taken into account for the resulting accelerations in the task space.

The same configuration as above is considered in the third case study, with a payload of 30 kg. It is clear from the plotted ellipsoid (Fig. 4) that in this case it is not possible to produce end-effector accelerations directed upwards when a payload is present. Furthermore, the set of torques satisfying eq. (9) subjected to the given torque limits cannot even ensure that the manipulator stands still. Notice that in this situation, the formulation proposed by [6] cannot be used since the ellipsoid cannot be defined at all.

In the fourth case study, the assigned configuration is $\mathbf{q} = (90 \ -90)^T$ deg and a payload of 5 kg is considered (Fig. 5). This configuration evidences that the translation of the ellipsoid's center is directed exactly downwards. This is a particular situation since in general — as it occurs in the other examples — the geometrical constraints between the different masses produce end-effector accelerations with both components different from zero.

In the fifth and last case study, for the sake of completeness, a redundant three-degree-of-freedom planar manipulator is considered. The parameters are (in SI units): $\ell_1 = 0.50$, $\ell_2 = 0.73$, $\ell_3 = 0.20$, $\ell_{c1} = 0.205$, $\ell_{c2} = 0.320$, $\ell_{c3} = 0.023$, $m_1 = 56.5$, $m_2 = 28.7$, $m_3 = 5.2$, $I_1 = 2.58$, $I_2 = 1.67$, $I_3 = 0.0125$, $f_{1,\max} = 1890$, $f_{2,\max} = 540$, $f_{3,\max} = 160.5$. These parameters correspond to the planar structure (joints 2, 3 and 5) of the MANUTEC R3 manipulator [11]. The maximum allowed payload of 15 kg is considered. In Fig. 6 the ellipsoids obtained in the configuration $\mathbf{q} = (120 \ -90 \ -60)^T$ deg are presented.

4. Conclusions

This paper has established a new formulation of the dynamic manipulability ellipsoid for robotic manipulators. Differently from the original formulation, it has been demonstrated that the effects of arm and payload gravitational forces are not to produce a contraction of the size of the ellipsoid, but only a translation of its center with respect to the reference frame in which the ellipsoid is defined. A number of case studies have been developed to the purpose of evidencing this property and thoroughly understanding the influence of link and payload mass distributions on the size and location of the ellipsoid. The concept has also been applied to the relevant case of redundant manipulators; in this case it is possible to devise resolution algorithms which achieve arm reconfiguration by suitably exploiting dexterity indices based on the proposed ellipsoid. As an aside, we have extended the formulation to cooperative manipulators that present the same kind of manipulability issues [12].

Acknowledgements

This work was supported by *Consiglio Nazionale delle Ricerche* under contract 90.00400.PF67.

References

- [1] T. Yoshikawa, "Analysis and control of robot manipulators with redundancy," in *Robotics Research: The 1st International Symposium*, eds. M. Brady and R. Paul, MIT Press, Cambridge, MA, pp. 735-747, 1984.
- [2] T. Yoshikawa, "Manipulability of robotic mechanisms," *International Journal of Robotics Research*, vol. 4, no. 2, pp. 3-9, 1985.
- [3] S.L. Chiu, "Task compatibility of manipulator postures," *International Journal of Robotics Research*, vol. 7, no. 5, pp. 13-21, 1988.
- [4] C.A. Klein and B.E. Blaho, "Dexterity measures for the design and control of kinematically redundant manipulators," *International Journal of Robotics Research*, vol. 6, no. 2, pp. 72-83, 1987.
- [5] T. Yoshikawa, "Translational and rotational manipulability of robotic manipulators," *Proceedings of the 1990 American Control Conference*, San Diego, CA, pp. 228-233, May 1990.
- [6] T. Yoshikawa, "Dynamic manipulability of robot manipulators," *Journal of Robotic Systems*, vol. 2, pp. 113-124, 1985.
- [7] H. Asada, "A geometrical representation of manipulator dynamics and its application to arm design," *Transactions of the ASME Journal of Dynamic Systems, Measurement, and Control*, vol. 105, pp. 131-142, 1983.
- [8] V.D. Tourassis and C.P. Neuman, "The inertial characteristics of dynamic robot models," *Mechanism and Machine Theory*, vol. 20, pp. 41-52, 1985.
- [9] T.J. Graettinger and B.H. Krogh, "The acceleration radius: A global performance measure for robotic manipulators," *IEEE Journal of Robotics and Automation*, vol. RA-4, pp. 60-69, 1988.
- [10] O. Ma and J. Angeles, "The concept of dynamic isotropy and its applications to inverse kinematics and trajectory planning," *Proceedings of the 1990 IEEE International Conference on Robotics and Automation*, Cincinnati, OH, pp. 481-486, May 1990.
- [11] M. Otter and S. Türk, *The DFVLR Models 1 and 2 of the Manutec R3 Robot*, DFVLR-Mitteilung 88-13, 1988.
- [12] P. Chiacchio, S. Chiaverini, L. Sciavicco, and B. Siciliano, "Task-space dynamic analysis of multi-arm system configurations," *International Journal of Robotics Research*, to appear, 1991.

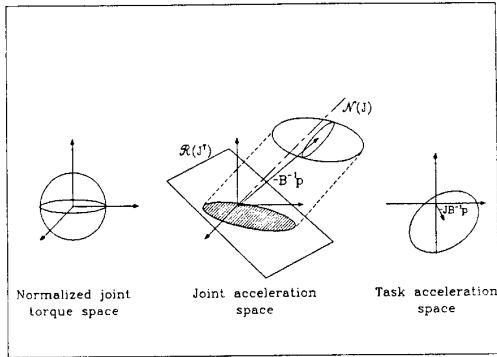


Fig. 1 Example of ellipsoids mapping for a redundant arm.

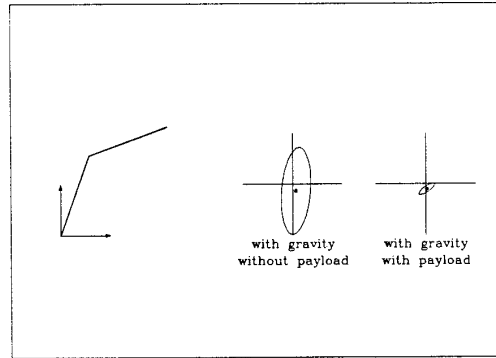


Fig. 4 Dynamic ellipsoids for case study # 3.

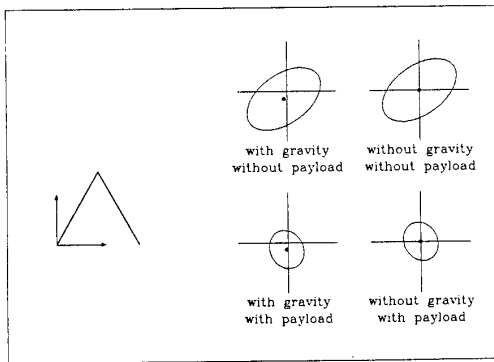


Fig. 2 Dynamic ellipsoids for case study # 1.

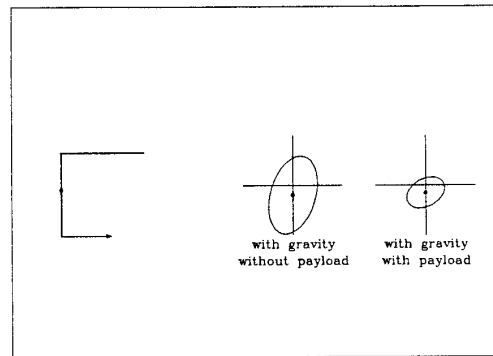


Fig. 5 Dynamic ellipsoids for case study # 4.

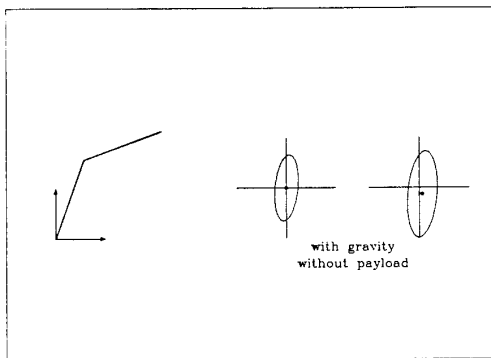


Fig. 3 Dynamic ellipsoids for case study # 2 — left: method in [6]; right: our method.

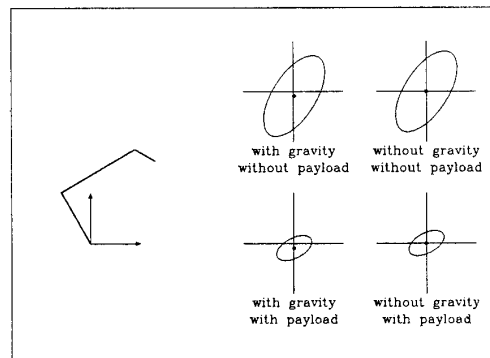


Fig. 6 Dynamic ellipsoids for case study # 5.